IN SITU SOIL RESPONSE DURING VIBRO-REPLACEMENT

Ali Amini, The University of British Columbia, Vancouver, BC
John A. Howie, The University of British Columbia, Vancouver, BC
Nelson Beaton, Geopac West Ltd., Vancouver, BC

ABSTRACT
Deep vibrocompaction methods such as vibroflotation have been around for more than 70 years and have proved to be effective in compaction of granular soils. However, the mechanism of densification and the soil-vibrator interaction are not clearly understood. This paper presents the results of continuous monitoring of vibrator and ground response during construction of 5 stone columns in a vibro-replacement project. Time histories of three components of acceleration were recorded on the VFAG-V23 vibrator and in the ground. Time histories of pore pressures were also recorded in the ground. These data were collected in conjunction with the time variation of power consumption of the electrical motor and depth. The vibrator and ground vibrated at the same frequency (29 Hz), close to the resonant frequency of the system of 26 Hz, with horizontal motion being predominant. Attenuation of horizontal acceleration with radial distance was approximately consistent with spherical spreading while vertical accelerations attenuated more slowly. The relative significance of tangential and radial accelerations was observed to be dependent on the radial distance from the vibrator. At a radial distance of 1.7m, the tangential accelerations were found to be predominant, while radial accelerations were equally significant at greater distances.

RÉSUMÉ
Les méthodes de vibro-compaction profond comme la vibroflotation a été utilisé pour plus de 70 ans et a été prouvée effective dans la compaction du sols granules. Cependant, le mecanisme de densification et l'interaction de sol-vibrateur ne sont pas bien compris. Cet article présente les résultants de la surveillance continue de la vibrateur et du sol pendant la construction de cinq colonnes de Pierre dans un projet de vibro-replacement. Les histoires du temps de trois composants d'accélération a été noté dans la VFAG-V23 vibrateur et dans le sol. Les histoires de temps de la pression interstitielle a été note aussi. Ces données ont été ramassées conjointement avec la variation de la consommation d'énergie du moteur électrique et avec la profondeur. La vibrateur et le sol ont vibré a la même fréquence (29 Hz), qui est près de la fréquence résonante du système (26 Hz). Le mouvement horizontal a été prédominant. L'atténuation de l'accélération horizontale avec la distance radiale a été approximativement consistent avec la propagation sphericale, tandis que l'atténuation de l'accélérations verticales a été plus lente. L'importance relative de l'accélérations tangentielles et radiales a été observé être dépendant de la distance radiale de la vibrateur. A la distance radiale de 1.7 m, l'accélérations tangentielles ont été prédominantes, tandis que l'accélérations radiales ont été aussi importantes aux distances plus grandes.

1. INTRODUCTION

In the preface to the first Geotechnique symposium on ground improvement, Burland et al. (1976) noted that that there was a mystique surrounding ground treatment techniques. About 30 years later, Charles (2002) noted that "an improved understanding of the physical treatment process through numerical analysis and testing of physical models would be beneficial."

Vibroflotation has been used for about 70 years and has proved to be effective in compaction of granular soil. However, very little can be found in the literature on field vibration measurement (i.e. Baez and Martin, 1992; Morgan and Thomson, 1983), laboratory small scale model testing (i.e. Metzger and Koerner, 1975), theoretical analysis (Fellin, 2000) and almost none on its numerical analysis. The main reason for this scarcity is the complexity of the process.

In response to this need, research was initiated to provide a better understanding of the physical treatment process. This included field vibration measurement, numerical analysis and interpretation of in situ testing after improvement. This paper presents the results of field monitoring of vibration and ground response during a vibro-replacement project and then discusses some of the main observations such as frequency response, vibration attenuation, mechanism of compaction and mechanism of vibrator penetration.

2. WET VIBRO-REPLACEMENT TECHNIQUE

Wet vibro-replacement is a densification method in which a down-hole vibrator (Figure 1) with centrifugal vibration is inserted into the ground with the help of water and/or air jetted from its nose and side jets. Excess pore pressure caused by the combination of vibration and jetting, and dynamic instability due to high acceleration reduces soil resistance and allows the vibrator to penetrate into the ground under its own weight. Once the target depth is reached, and after typically one or more cycles of flushing of the hole, the backfilling process starts from the bottom

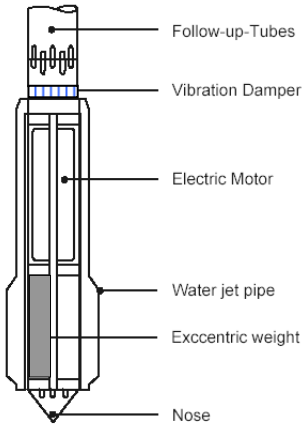

Figure 1- Cross-section of a Vibroflot
(From website www.vibroflotation.com)

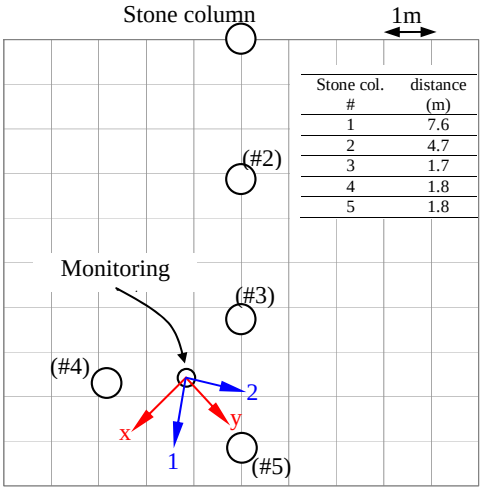

Stone col. #	distance (m)
1	7.6
2	4.7
3	1.7
4	1.8
5	1.8

Figure 2- Site plan- Monitored stone columns

up. The vibrator is withdrawn slowly, usually in half-metre intervals, while crushed rock is fed from the surface to the bottom of the hole. It passes through the annulus opened up between the soil and vibrator unit by flushing cycles and the side jets. The vibrator is held at each interval for a predetermined amount of time or until a specified power consumption is reached. Lateral movements of the vibrator, created by centrifugal forces due to rotation of an eccentric mass, are transferred to the soil. Furthermore, the tendency of the vibrator to spin about its vertical axis is resisted by fins protruding from its sides. This imparts torsional vibrations to the soil. The soil is compacted primarily by the large number of cycles of shear strain as well as by consolidation under the imposed increase in lateral stress. Coupling between soil and vibrator is enhanced by the introduction of stone to the annular zone around the vibrator. Stone columns are usually arranged in a triangular or square grid pattern and the overall improvement is achieved by a combination of densification, reinforcement and probably an enhanced drainage condition.

3. FIELD MEASUREMENT OF INPUT VIBRATION AND RESPONSE

Installation of five stone columns was monitored as part of a vibro-replacement project in Richmond, B.C., Canada. The soil profile, typical of the Fraser River Delta, consisted of 5 m of clayey silt underlain by 1.5 m of sandy silt to silty sand which, in turn, was underlain by fine to medium sand to silty sand up to about 13 m depth. The ground treatment was intended to improve the resistance to seismic shaking of these layers. 10 m deep stone columns were installed at 3 m centres in a triangular pattern. Figure 2 shows the location at which ground response and pore pressure time histories were monitored. The numbers beside the stone columns indicate the sequence of their construction. The following data were gathered versus time during monitoring of construction of the five stone columns:

- 3-axis accelerations at 0.7 m above the nose of the vibroflot.
- Current drawn by the electric motor of the vibroflot.
- Depth of the vibroflot.
- 3-axis vibration of the ground at 8.5m depth.
- Pore water pressure of the soil at 8.5m depth.

A Vibroflot model VFAG-V23 was used. This vibrator operates at ~1800 rpm, has a 130 kW electric motor and produces 300 KN of centrifugal force.

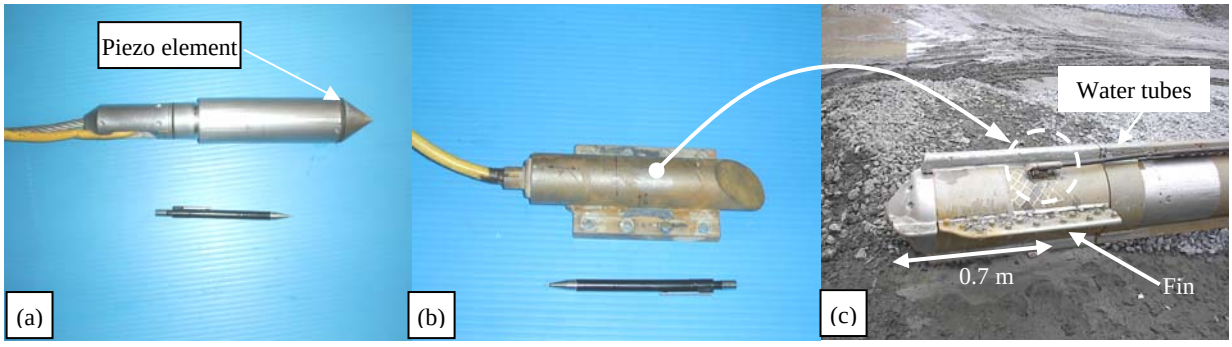

Figure 3- Vibration monitoring equipment, (a) sensor package in the ground, (b) & (c) sensor package on the vibroflot

3.1 Vibration measurement equipment

Two sensor packages, designed and built at the University of British Columbia (UBC), were used to monitor the vibration of the vibrator and ground. The sensor package for monitoring ground vibration consisted of 3 orthogonal accelerometers and one pore pressure transducer as shown in Figure 3-a. IC Sensors model 3031 piezo-resistive accelerometers were used. These have a range of +/- 10g, a frequency response range of 0-600 Hz and a mounted resonant frequency of 1200Hz. They were mounted rigidly in a steel cone shaped housing, about 300mm long and 45 mm in diameter. The pore pressure transducer had a capacity of 350 kPa and was manufactured by Sensym ICT. The package was installed at 8.5 m depth using 45 mm OD rods, pushed using the UBC in situ research vehicle. The rods were then detached from the instrumentation housing and withdrawn. This was to eliminate the effect of the pushing rods on the measured vibration. Great care was taken to prevent the sensor package from rotating during installation. A 10 mm steel cable attached to the package allowed recovery of the instrument after completion of monitoring.

The motion of the vibroflot was monitored using an accelerometer package as shown in Figure 3-b. The package consisted of three orthogonal accelerometers and an amplifier board. Down-hole amplification of signals was necessary to increase the signal to noise ratio as the cable carrying the signals passed through the strong electromagnetic field of the electric motor in the vibroflot. The accelerometers used were the same as in the ground package but with higher capacity. They had a range of +/- 50g, a frequency response range of 0 to 1050 Hz and a mounted resonant frequency of 1800 Hz. The steel package housing was 200mm long, 35mm in diameter and was bolted on a plate which was then welded to the vibroflot wear jacket, 0.7 m above the nose (Figure 3-c). The electric cable was guided through a ½ " steel pipe all the way up to the top of the extension tubes, over a pulley and then to the data acquisition computer. The package had to be very robust as it experienced a very rough environment and high impacts.

The time histories of vibration were recorded at a sampling rate of 333 Hz using an EGAA data acquisition system developed by RC Electronics Inc. This was the maximum sampling rate that could support simultaneous recording of 7 channels. This rate was considered to be adequate as about 11 data points were recorded for each cycle of vibration at the predominant frequency of 29 Hz.

3.2 Results of vibration measurement

Figure 4 shows time histories of the measured parameters in the ground and on the vibroflot along with the depth of the vibroflot nose and its power consumption during construction of stone column #3. The horizontal ground accelerations were measured in the direction of the active axes of the horizontal accelerometers. These are axes 1 and 2 in Figure 2. These horizontal accelerations were

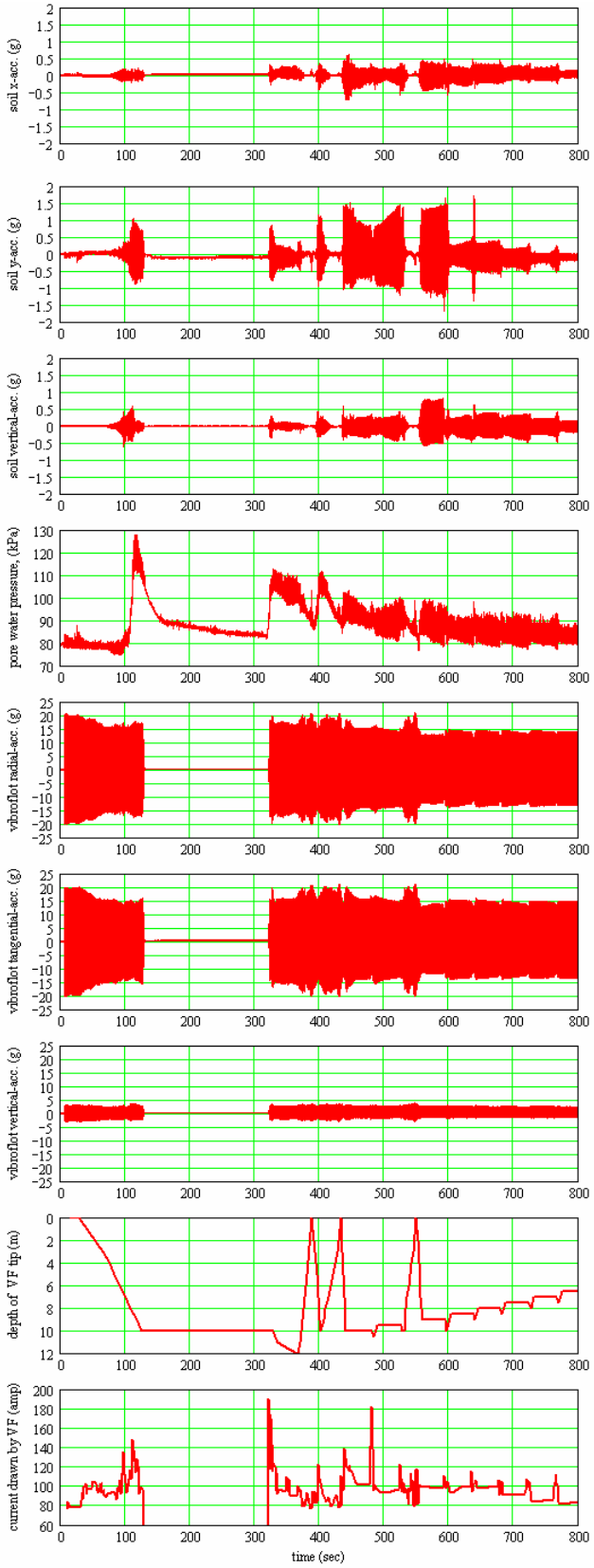

Figure 4- Recorded time histories during stone column #3

then transformed to the local coordination system with axes radial and tangential (x and y respectively) to stone column #3. In Figure 2, the local coordinate system is shown only for stone column #3 for clarity.

It may be observed from Figure 4 that the vibroflot was turned on at t=5 sec while hanging in the air. At t=30 sec, the vibroflot started penetrating the ground and took about 90 sec to reach the target depth of 10 m. At this point, the vibroflot and water jets were turned off to monitor the pore water pressure response of the ground. Note that this is not the conventional procedure. After about 200 sec, the water jets and vibroflot were turned on again. The hole was flushed twice before densification began at about 440 sec at 10 m depth. The operator then worked his way up in 0.5 m depth increments. During the first flushing, the first load of crushed rocks was deposited into the hole by a wheel loader.

Due to the time scale, data presented in Figure 4 are compressed and only show the maximum and minimum envelopes. Figure 5 is a portion of the time histories during densification showing the full signals. The motion of vibroflot is sinusoidal whereas the ground responses are periodic but irregular. Radial acceleration (acc-x) and pore pressure signals (not shown here) are the most irregular. It is likely that the interaction between the vibrator and the stones around it generates higher frequency ground motions that contribute to this irregularity.

4. DISCUSSION

The data in Figure 4 contain a large amount of information. In this section, some of the main observations are highlighted and explained and, whenever possible, are compared with the results of previous studies.

4.1 Frequency analysis of the time histories

Figure 6 shows the frequency analysis of the input and out put vibration. The predominant frequencies of vibration for vibrator and ground response are the same (about 29 Hz). A forced vibration system at steady state should vibrate at the frequency of excitation. The predominant frequency remains constant throughout the process and is independent of the ground condition around the vibrator.

4.2 Attenuation of vibration

Attenuation of vibration in the ground is due to geometric spreading and material damping and could be represented by the following Equation 1.

$$\frac{A_2}{A_1} = \left(\frac{r_1}{r_2}\right)^n . e^{-\alpha(r_2 - r_1)} . \frac{1}{T} \qquad [1]$$

where A_1 and A_2 are amplitudes at distances r_1 and r_2 from the source of vibration respectively. n is a coefficient representing the geometric spreading; n=0 for rods and plane waves, n=0.5 for cylindrical wave fronts and n=1 for spherical wave front. α is an empirical coefficient, which depends on damping and stiffness of the ground as well as the vibration frequency. If the propagating wave encounters interfaces, then partial transmission/reflection of energy and mode conversion occurs, which is presented by T in the above equation.

Figure 7a illustrates the attenuation of the maximum radial and tangential accelerations measured at different distances from the vibroflot during backfilling and densification phase, where the vibroflot and the accelerometers in the ground were at the same depth. Also shown for comparison are the radial accelerations from a bottom feed "S" type Keller vibrator of 120 kW power and 200 KN centrifugal force operating at 30 Hz (Baez and Martin 1992). They used a seismic cone for vibration measurement. The presence of the stiff cone rods might be expected to have an effect on the measurements but both sets of data show similar trends of vibration attenuation for radial vibration. Close to the vibrator, the tangential acceleration was observed to be considerably larger than the radial acceleration. This parameter was not monitored b y Baez and Martin (1992).

Figure 7b shows the attenuation of resultant horizontal acceleration (square root of the sum of square of radial and tangential accelerations) with distance. Also shown are the theoretical attenuation curves assuming spherical attenuation with different α values. The effect of partial transmission and mode conversion is ignored here. It may

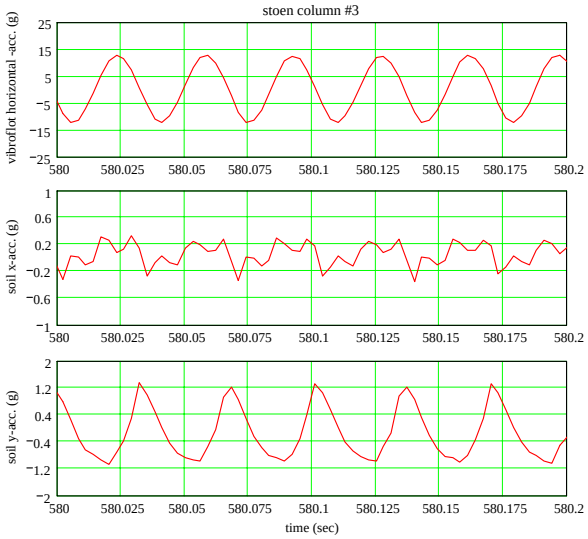

Figure 5- Vibration time histories during densification

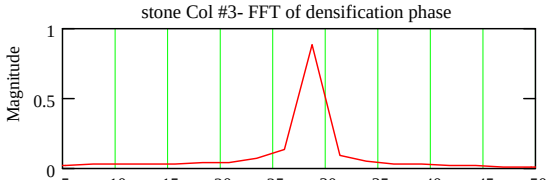

Figure 6- Frequency spectra of acceleration time histories of vibroflot and ground during densification

be observed that an average α=5% fits the data. This is in the range of α values reported by Woods and Jedele (1985) for sandy soils.

As shown in Figure 7c, vertical acceleration in the ground attenuates proportional to $1/r^{0.79}$. This attenuation rate is between cylindrical and spherical attenuation. This could be because vertical excitation is transmitted to the ground over a longer length and the source is between a line source and a point source.

4.3 Optimal frequency of vibration

Massarsch and Heppel (1991) noted that vibration at an optimal input frequency, at which the response of the ground peaks, results in higher particle motion and better densification. They suggested that the optimal frequency of the vibrator can be found by monitoring the system response during switch off or switch on of the vibrator. At these times, all the frequencies from zero to the operating frequency are swept and the optimal frequency is the one corresponding to the maximum ground response.

Figure 8 shows the vibration of the vibroflot and the horizontal accelerations of the ground after switch on at t~322 sec, enlarged from Figure 4. In Fig. 8, the ground response peaks before reaching the maximum frequency at steady state. This is despite the fact that the impact force at this optimal frequency is lower than that at the steady state as the impact force is a function of the square of the frequency. Figure 9 shows the ratio of the ground acceleration to vibroflot acceleration versus frequency at three different times during the transient state. The vibration frequency corresponding to the peak response is about 26 Hz. The operating frequency of 29 Hz is close to the optimal frequency for this site. It should be noted that the optimal frequency depends on the soil conditions and should increase with densification.

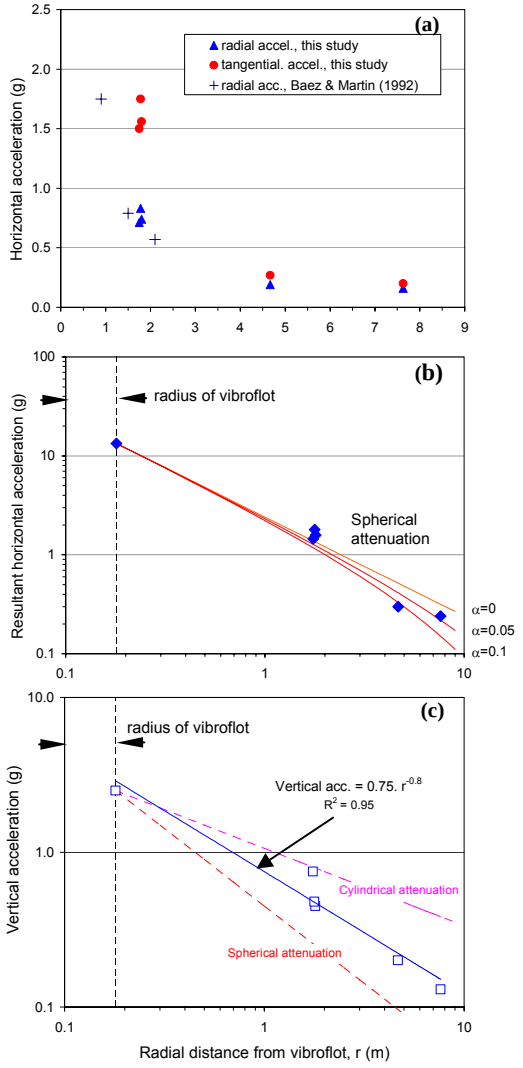

Figure 7- Attenuation of ground accelerations, a) horizontal radial & tangential, b) resultant horizontal, c) vertical

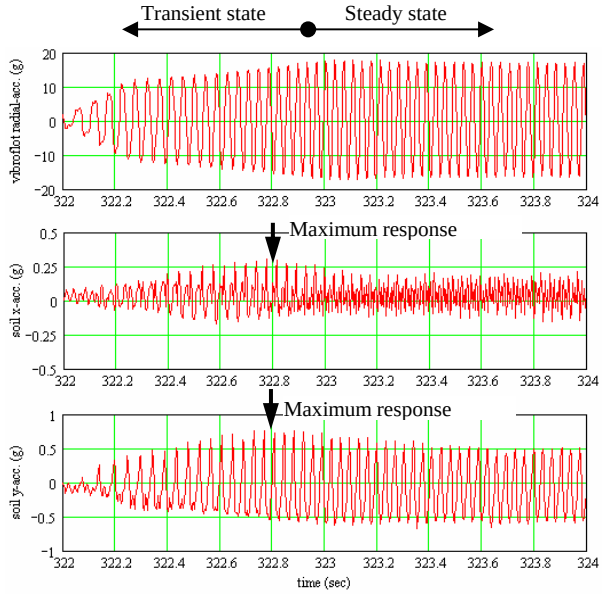

Figure 8- Response of the vibroflot (top) and ground (mid. & bot.) during switch on, (enlarged from Fig. 4)

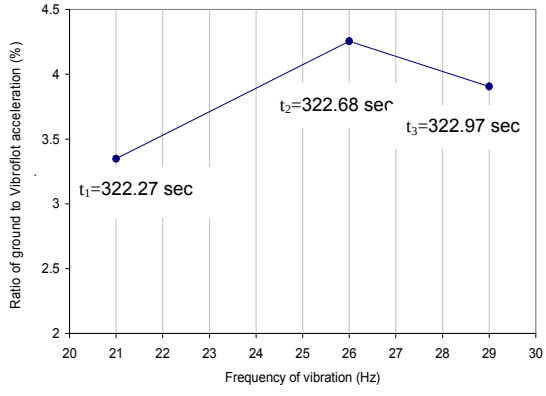

Figure 9- Response of the vibroflot and ground during switch on, (enlarged from Fig. 4)

4.4 Horizontal motion path

The motion paths of the soil particles and the vibroflot were obtained by double integration of the acceleration time histories. Due to potential errors such as baseline shift that could be introduced by integration, we have chosen to demonstrate the shape of the motion path in terms of accelerations. Assuming a harmonic signal, which is the case for vibroflot motion, the shape of acceleration path and displacement path should be the same. This may not be exact for the soil particle motion. However, it serves the purpose of showing the relative significance of motion in the tangential and radial directions.

In Figure 10a it may be observed that the vibroflot has a circular horizontal motion in the air. The amplitude of motion of the vibroflot significantly decreases in the ground due to the confinement (Figure 10b). However it remains almost circular which is not consistent with the experiment of Morgan and Thomson (1983) who observed smaller particle motion normal to the plane of the fins. They attributed this to greater bearing area in this direction. In the study here, it is likely that the presence of the water tubes, that deliver water along the outside of the vibroflot to the nose water jets, has counterbalanced the effect of the fins (see Figure 3c).

Figure 10c, d and e illustrate the ground particle motion path during densification for stone columns #1 to 3. The motion path is a function of distance from the vibroflot. At a radius of 1.7 m, the acceleration is greater in the tangential direction. The same behavior was also observed from stone columns #4 and 5 at a horizontal distance of about 1.8m. Preliminary numerical modelling of the soil-vibrator interaction, not included in this paper, suggests that this phenomenon is real.

4.5 Densification phase

Figure 11 shows the vibroflot response, depth and amperage (electrical current consumption) during the densification phase. Due to symmetry, only the positive half of the acceleration is shown for more clarity. It is conventionally assumed that an increase in resistance of the ground around the vibroflot due to densification is indicated by increased amperage and decreased amplitude of vibroflot motion. These parameters are used for field quality control. The data presented here suggests that these parameters may not always be reliable indicators.

From 400 to 440 sec, the vibroflot was lifted up to the ground surface. The hole was kept open by the water jets and so the resistance of the soil against the vibrator was small. This resulted in low amperage and high vibroflot amplitude. After re-penetration to 10 m depth, the nose jets were turned off and densification began at 440 sec. It took about 10 sec for crushed stone and the surrounding ground to build up resistance and decrease the amplitude of the vibroflot. During this 10 sec, the amperage consumption also decreased. This is opposite to the usual

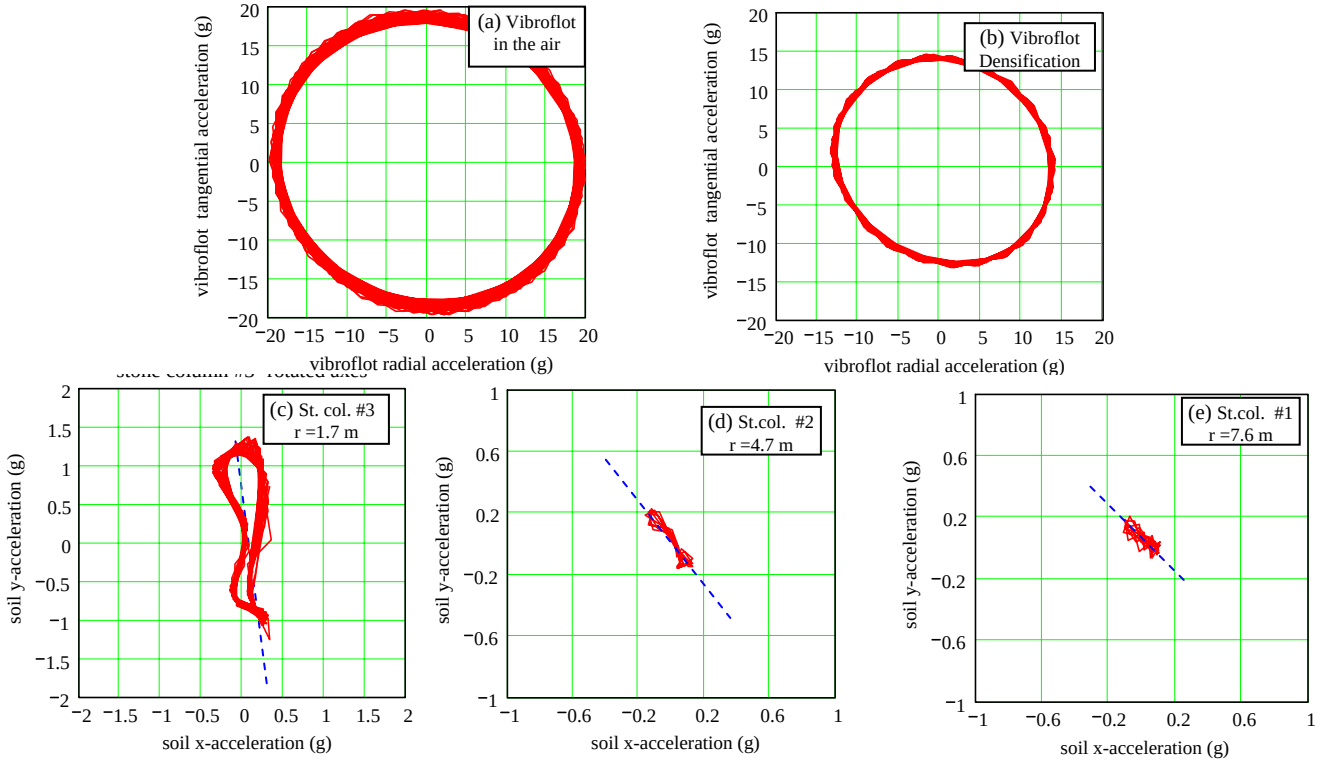

Figure 10- (a & b), Motion paths of the Vibroflot and (c, d & e), Motion path of ground at different distances from vibroflot during densification

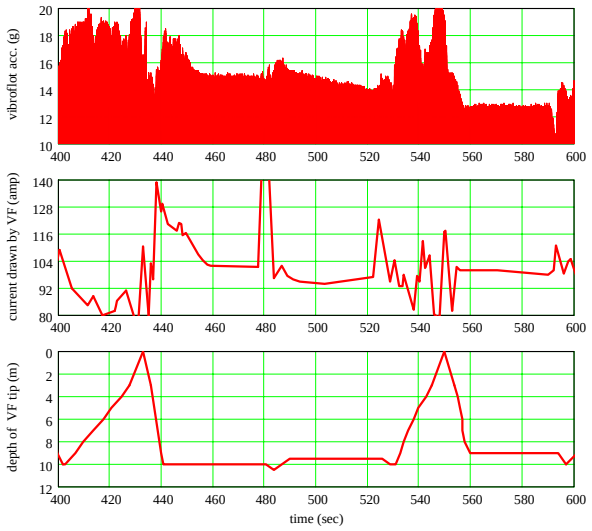

Figure 11- Densification phase (enlarged from Figure 4)

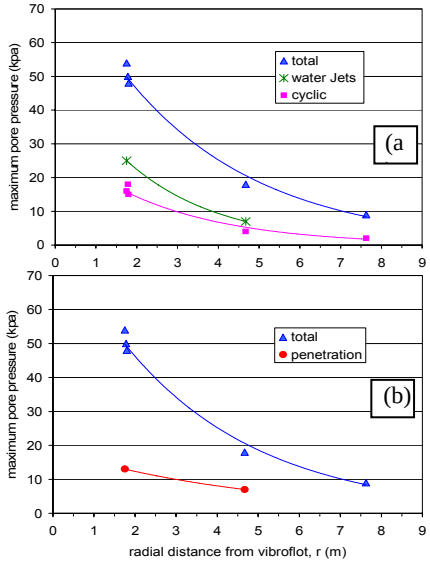

Figure 12- Pore pressure response during vibroflot penetration

trend. It should be noted that the amperage depends on the motion of the entire vibroflot and not only on the motion of the tip. The pivot point of the vibration moves further down from the vibration isolator when the vibroflot goes into the ground (Greenwood 1991). This causes greater motion of the vibroflot shoulder. The data indicate that the vibrator amplitude and amperage could show opposite trends due to complexity of the phenomenon. Based on local experience, a diminished amperage increase occurs when fines contents are in the range of 15-20% or more.

The above suggests that basing quality control of densification on interpretation of the amperage or vibroflot amplitude alone may not be sufficient as these factors are dependent on the methodology and the soil grain size distribution (i.e. fines content / drainage characteristics) of the soils being treated. Whereas Morgan and Thomson (1983) found good correlation between the post-compaction SPT blow counts and the vibroflot amplitude, Fellin (2000) suggested that measurement of the acceleration at the tip and shoulder of the vibroflot and also of the phase angle of the eccentric mass relative to the motion of the vibroflot could be used for online compaction control. This requires further research and field confirmation.

During densification, no residual increase of pore pressure was observed at the centroid. Most likely the rate of generation of the pore pressure during vibration is less than the rate of dissipation. However, there was a general dissipation of pore pressure between t=440sec and t=700sec. It is thought that this pore pressure is mainly due to the penetration of the vibroflot and also due to the side water jets that keep injecting water/pressure into the system.

4.6 Pore pressure response during penetration

Figure 12a shows the distribution of the pore pressure during the penetration phase of the vibroflot. The total excess pore pressure is the sum of the cyclic pore pressure, water pressure due to water jets and pore pressure generated from the cavity expansion by penetration of the vibroflot. During construction of stone columns #2 and #3, the vibroflot motor and water jets were turned off after penetration to the target depth. Then, after partial dissipation, the vibroflot and water jets were turned on. The sudden rise in pore pressure at this time (t ~320 sec in Figure 4) is from water jets and cyclic pore pressure. From this, the pore pressures due to water jets and the cavity expansion caused by penetration could be obtained as shown in Figure 12a and 12b. Extrapolation of excess pore pressure caused by water jets alone to small radii also gives pore pressures of about 60 kPa. This is about 70% of the initial effective vertical stress at 8.5m depth. These factors plus the scouring action of the nose water jets reduce the shear strength of the soil allowing the vibroflot to penetrate under its own weight with tip bearing pressures in the range of 0.5 MPa.

4.7 Mechanism of compaction

There is some confusion in the literature about the mechanism of compaction. Greenwood (1991) suggested that compaction would take place mainly where the acceleration was from 0.5g to 3g. This is based on Rodger (1979) who measured the acceleration at the ground surface. Baez and Martin (1992) suggested that vibration-induced liquefaction (pore pressure to initial effective stress ratio=1.0) during vibro-replacement would enhanced the process of densification. Note that the high pore pressure ratio occurred only during penetration and not during the densification phase and thus would not explain the main densification mechanism.

Data from cyclic laboratory tests have shown that compaction of granular soils is affected by the number and magnitude of cyclic shear strains (e.g. Youd, 1972)

experienced by the soil. Therefore, it would have been useful to measure shear strains in the ground. However, direct measurement of the shear strains in the field is difficult. Estimation of the magnitudes of shear strains using numerical modeling is the subject of current research.

5. SUMMARY AND CONCLUSIONS

In order to obtain a better understanding of the physical process of vibro-replacement and also to provide data for calibration of numerical analysis, field measurements of vibroflot vibration, as well as ground vibration and pore water pressure response were carried out during vibro-replacement. A preliminary assessment of the data presented above has resulted in the following conclusions. As expected in a forced vibration system, the ground vibrated with the same frequency as the vibrator (~29 Hz). This was close to the optimal frequency of 26 Hz, interpreted from the transient state of vibration during switch on.

The vibroflot acceleration was measured about 20g when freely suspended above the ground and reduced to 14g during the backfilling and densification phase. The vibrator generated mainly horizontal but also some vertical vibrations in the ground. The maximum steady state resultant horizontal acceleration was measured about 1.7g to 0.25g at radial distances of 1.7m to 7.6m, respectively. For the same locations, the maximum vertical acceleration varied from 0.6g to 0.13g. The data have been considered in comparison to idealized models of vibration. The horizontal vibration field around the probe appears to be matched by spherical attenuation whereas the vertical motions appear to attenuate more slowly.

The relative magnitude of radial and tangential acceleration in the ground was found to be dependent on the distance from the vibrator. At 1.7m away from the vibroflot, the tangential accelerations were greater than the radial accelerations. Extrapolation of excess pore water pressure due to water jets amounted to a large proportion of the initial vertical effective stress and significantly facilitated the vibroflot penetration.

In addition, it was shown that measurements of vibrator amplitude and power consumption could indicate contradictory trends and variable sensitivity to the details of the densification process. This suggests that additional performance indicators may be required to improve quality control of the densification process in the field.

Results of the field measurement was simulated in numerical model and provided considerable insight into the mechanism of ground densification. This will be discussed in a separate paper.

6. ACKNOWLEDGMENTS

The authors acknowledge the financial support of the Natural Science and Engineering Research Council of Canada, the GREAT Award program of the Science Council of B.C. and the industrial collaborators: Conetec Investigations Ltd., Geopac West Ltd., Foundex Explorations Ltd. and Klohn Crippen Consultants Ltd., , The assistance of the technical support staff of the University of British Columbia, Department of Civil Engineering in particular Scott Jackson and Harald Schrempp is greatly appreciated. Also thanks to Mike Jokic for translation of the abstract into French.

6.1 REFERENCES

Baez, J.I. and Martin, G.R. 1992. Liquefaction observations during installation of stone columns using the vibro-replacement technique, Geotechnical News Magazine, September 1992, pp. 41-44.

Burland, J.B., McKenna, J.M. and Tomlinson, M.J. 1976. Preface: Ground treatment by deep compaction, Geotechnique, 25, No.1, pp. 1-2.

Charles, J.A. 2002. Ground improvement: the interaction of engineering science and experience-based technology, Geotechnique, 52, No. 7, pp. 527-532.

Fellin, W. 2000. Quality control in deep vibrocompaction, In International workshop on compaction of soils, granulates and powders, (D. Kolymbas and W. Fellin eds.), Innsbruck, February 2000, pp. 133-144.

Greenwood, D.A., 1991. Vibrational loading used in the construction process, Chapter 10, Cyclic loading of soils: from theory to design (O'Reilly and Brown, eds.), Blackie and Son Ltd. pp. 435-475.

Massarsch, K. R. and Heppel, G. 1991. Deep vibratory compaction using Muller Resonance Compaction (MRC) system, Report 91:2, Muller Geosystems, Mafburg, Germany, 23 pp.

Metzger, G.V. and Koerner, R.M. 1975. Modeling of soil densification by vibroflotation, Journal of Geotechnical Engineering Division, ASCE, Vol. 101, No. GT4, pp. 417-421.

Morgan, J.G.D. and Thomson, G.H. 1983. Instrumentation methods for control of ground density in deep vibrocompaction, In Proceeding of the 8th European Conference on Soil Mechanics and Foundation Engineering, Helsinki, pp. 59-64.

Youd, T.L. 1972. Compaction of sands by repeated shear straining. Journal of Soil Mechanics and Foundations Div., ASCE, 98 (7), pp. 709-725.